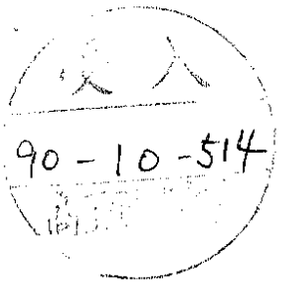


EUROPEAN ORGANIZATION FOR NUCLEAR RESEARCH

CERN-PPE/90-143
ERRATUM
November 14, 1990

# "A Study of the Recombination Scheme Dependence of Jet Production Rates and of $\alpha_s(M_{Z^0})$ in Hadronic $Z^0$ Decays"

The OPAL Collaboration

Due to an inconsistency between our $O(\alpha_s^2)$ QCD fitting program and the calculations of Kunszt and Nason [1], the $\alpha_s$ values quoted in CERN-PPE/90-143 [2] are systematically too small by about 2.5 to 3 %. The correct treatment of these calculations thus alters the final result from $\alpha_s(M_{Z^0}) = 0.115 \pm 0.008$, as quoted in [2], to

$$\alpha_s(M_{Z^0}) = 0.118 \pm 0.008,$$

which corresponds to $\Lambda^{(5)}_{\overline{MS}} = 225^{+120}_{-85}$MeV, where the error includes all experimental and theoretical uncertainties as described in [2].

The actual fit results of $\Lambda_{\overline{MS}}$, the renormalisation scale factor $f$, of $\alpha_s(M_{Z^0})$ and its systematic uncertainties are updated in Tables 6 and 8 below, which should replace the corresponding tables in [2]. These values should also replace the respective numbers presented in the text and in Fig. 3. The theoretical curves shown in Fig. 3, as well as the data in general, remain unchanged.

Apart from an overall change of all $\alpha_s$ values by +0.003, the data analysis and overall conclusions presented in [2] remain unchanged. We are grateful to G. Turnock for pointing out the inconsistency in our program.

| Fit | E0-scheme | E-scheme | p0-scheme | p-scheme |
|---|---|---|---|---|
| $\Lambda_{\overline{MS}}$ ($f$=1) | $330^{+51}_{-47}$ | $718^{+97}_{-91}$ | $267^{+52}_{-47}$ | $247^{+44}_{-39}$ |
| $\Lambda_{\overline{MS}}$ | $147^{+18}_{-16}$ | $143 \pm 15$ | $191^{+26}_{-23}$ | $200^{+50}_{-25}$ |
| $f$ | $0.0052^{+0.0024}_{-0.0013}$ | $0.00006 \pm 0.00001$ | $0.090^{+0.290}_{-0.053}$ | $0.19^{+1.18}_{-0.19}$ |

**Table 6.** Fit results of $\Lambda_{\overline{MS}}$ for fixed renormalisation scale factor $f = \mu^2/E^2_{cm} \equiv 1$ and for the simultaneous determination of $\Lambda_{\overline{MS}}$ and $f$ in the differential $D_2$ distributions.

| Scheme | $\alpha_s(M_{Z^0})$ | $\Delta\alpha_s$ (exp.) | $\Delta\alpha_s$ (had.) | $\Delta\alpha_s$ ($Q_0$) | $\Delta\alpha_s$ (scale) | $\Delta\alpha_s$ (tot.) |
|---|---|---|---|---|---|---|
| E0 | 0.118 | $\pm$0.003 | $\pm$0.003 | $\pm$0.003 | $\pm$0.007 | $\pm$0.009 |
| E | 0.126 | $\pm$0.003 | $\pm$0.003 | $\pm$0.003 | $\pm$0.013 | $\pm$0.014 |
| p0 | 0.118 | $\pm$0.003 | $\pm$0.003 | $\pm$0.005 | $\pm$0.004 | $\pm$0.008 |
| p | 0.118 | $\pm$0.003 | $\pm$0.003 | $\pm$0.006 | $\pm$0.003 | $\pm$0.008 |

**Table 8.** Final results of $\alpha_s(M_{Z^0})$ for different recombination schemes.

[1] Z.Kunszt and P.Nason [conv.], in "Z Physics at LEP 1" (eds. G.Altarelli, R.Kleiss and C.Verzegnassi ), CERN 89-08 (1989).

[2] OPAL collab., M.Z. Akrawy et al., CERN-PPE/90-143.

EUROPEAN ORGANIZATION FOR NUCLEAR RESEARCH

CERN-PPE/90-143
October 1, 1990

# A Study of the Recombination Scheme Dependence of Jet Production Rates and of $\alpha_s(M_{Z^0})$ in Hadronic $Z^0$ Decays

The OPAL Collaboration

## Abstract

Jet production rates in hadronic $Z^0$ decays are studied using four different recombination schemes to define resolvable jets. The strong coupling constant $\alpha_s(M_{Z^0})$ is determined in fits of the corresponding $O(\alpha_s^2)$ QCD calculations to the differential 2-jet distributions $D_2(y)$. Hadronisation corrections and renormalisation scale uncertainties are found to be different for each recombination scheme. Within their overall systematic uncertainties, the four schemes yield consistent values of $\alpha_s(M_{Z^0})$, leading to a final result of

$$\alpha_s(M_{Z^0}) = 0.115 \pm 0.008.$$

The error includes the experimental uncertainties ($\pm 0.003$), uncertainties of hadronisation corrections and of the degree of parton virtualities to which the data are corrected, as well as the uncertainty of choosing the renormalisation scale.

(Submitted to Zeitschrift für Physik C)

# The OPAL Collaboration


M.Z. Akrawy[11], G. Alexander[21], J. Allison[14], P.P. Allport[5], K.J. Anderson[8], J.C. Armitage[6], G.T.J. Arnison[18], P. Ashton[14], G. Azuelos[16,f], J.T.M. Baines[14], A.H. Ball[15], J. Banks[14], G.J. Barker[11], R.J. Barlow[14], J.R. Batley[5], A. Beck[21], J. Becker[9], T. Behnke[7], K.W. Bell[18], G. Bella[21], S. Bethke[10], O. Biebel[3], U. Binder[9], I.J. Bloodworth[1], P. Bock[10], H. Breuker[7], R.M. Brown[18], R. Brun[7], A. Buijs[7], H.J. Burckhart[7], P. Capiluppi[2], R.K. Carnegie[6], A.A. Carter[11], J.R. Carter[5], C.Y. Chang[15], D.G. Charlton[7], J.T.M. Chrin[14], P.E.L. Clarke[23], I. Cohen[21], W.J. Collins[5], J.E. Conboy[13], M. Couch[1], M. Coupland[12], M. Cuffiani[2], S. Dado[20], G.M. Dallavalle[2], P. Debu[19], M.M. Deninno[2], A. Dieckmann[10], M. Dittmar[4], M.S. Dixit[17], E. Duchovni[24], I.P. Duerdoth[7,d], D.J.P. Dumas[6], P.A. Elcombe[5], P.G. Estabrooks[6], E. Etzion[21], F. Fabbri[2], P. Farthouat[19], H.M. Fischer[3], D.G. Fong[15], M.T. French[18], C. Fukunaga[22], A. Gaidot[19], O. Ganel[24], J.W. Gary[10], J. Gascon[16], N.I. Geddes[18], C.N.P. Gee[18], C. Geich-Gimbel[3], S.W. Gensler[8], F.X. Gentit[19], G. Giacomelli[2], V. Gibson[5], W.R. Gibson[11], J.D. Gillies[18], J. Goldberg[20], M.J. Goodrick[5], W. Gorn[4], D. Granite[20], E. Gross[24], J. Grunhaus[21], H. Hagedorn[9], J. Hagemann[7], M. Hansroul[7], C.K. Hargrove[17], I. Harrus[20], J. Hart[5], P.M. Hattersley[1], M. Hauschild[7], C.M. Hawkes[7], E. Heflin[4], R.J. Hemingway[6], R.D. Heuer[7], J.C. Hill[5], S.J. Hillier[1], C. Ho[4], J.D. Hobbs[8], P.R. Hobson[23], D. Hochman[24], B. Holl[7], R.J. Homer[1], S.R. Hou[15], C.P. Howarth[13], R.E. Hughes-Jones[14], R. Humbert[9], P. Igo-Kemenes[10], H. Ihssen[10], D.C. Imrie[23], L. Janissen[6], A. Jawahery[15], P.W. Jeffreys[18], H. Jeremie[16], M. Jimack[7], M. Jobes[1], R.W.L. Jones[11], P. Jovanovic[1], D. Karlen[6], K. Kawagoe[22], T. Kawamoto[22], R.G. Kellogg[15], B.W. Kennedy[13], C. Kleinwort[7], D.E. Klem[17], G. Knop[3], T. Kobayashi[22], T.P. Kokott[3], L. Köpke[7], R. Kowalewski[6], H. Kreutzmann[3], J. Kroll[8], M. Kuwano[22], P. Kyberd[11], G.D. Lafferty[14], F. Lamarche[16], W.J. Larson[4], J.G. Layter[4], P.Le Du[19], P. Leblanc[16], A.M. Lee[15], M.H. Lehto[13], D. Lellouch[7], P. Lennert[10], L. Lessard[16], L. Levinson[24], S.L. Lloyd[11], F.K. Loebinger[14], J.M. Lorah[15], B. Lorazo[16], M.J. Losty[17], J. Ludwig[9], J. Ma[4,b], A.A. Macbeth[14], M. Mannelli[7], S. Marcellini[2], G. Maringer[3], A.J. Martin[11], J.P. Martin[16], T. Mashimo[22], P. Mättig[7], U. Maur[3], T.J. McMahon[1], J.R. McNutt[23], F. Meijers[7], D. Menszner[10], F.S. Merritt[8], H. Mes[17], A. Michelini[7], R.P. Middleton[18], G. Mikenberg[24], J. Mildenberger[6], D.J. Miller[13], C. Milstene[21], M. Minowa[22], W. Mohr[9], A. Montanari[2], T. Mori[22], M.W. Moss[14], P.G. Murphy[14], W.J. Murray[5], B. Nellen[3], H.H. Nguyen[8], M. Nozaki[22], A.J.P. O'Dowd[14], S.W. O'Neale[7,e], B.P. O'Neill[4], F.G. Oakham[17], F. Odorici[2], M. Ogg[6], H. Oh[4], M.J. Oreglia[8], S. Orito[22], J.P. Pansart[19], G.N. Patrick[18], S.J. Pawley[14], P. Pfister[9], J.E. Pilcher[8], J.L. Pinfold[24], D.E. Plane[7], B. Poli[2], A. Pouladdej[6], E. Prebys[7], T.W. Pritchard[11], G. Quast[7], J. Raab[7], M.W. Redmond[8], D.L. Rees[1], M. Regimbald[16], K. Riles[4], C.M. Roach[5], S.A. Robins[11], A. Rollnik[3], J.M. Roney[8], S. Rossberg[9], A.M. Rossi[2,a], P. Routenburg[6], K. Runge[9], O. Runolfsson[7], S. Sanghera[6], R.A. Sansum[18], M. Sasaki[22], B.J. Saunders[18], A.D. Schaile[9], O. Schaile[9], W. Schappert[6], P. Scharff-Hansen[7], S. Schreiber[3], J. Schwarz[9], A. Shapira[24], B.C. Shen[4], P. Sherwood[13], A. Simon[3], P. Singh[11], G.P. Siroli[2], A. Skuja[15], A.M. Smith[7], T.J. Smith[1], G.A. Snow[15], R.W. Springer[15], M. Sproston[18], K. Stephens[14], H.E. Stier[9], R. Stroehmer[10], D. Strom[8], H. Takeda[22], T. Takeshita[22], P. Taras[16], N.J. Thackray[1], T. Tsukamoto[22], M.F. Turner[5], G. Tysarczyk-Niemeyer[10], D. Van den plas[16], G.J. VanDalen[4], G. Vasseur[19], C.J. Virtue[17], H. von der Schmitt[10], J. von Krogh[10], A. Wagner[10], C. Wahl[9], J.P. Walker[1], C.P. Ward[5], D.R. Ward[5], P.M. Watkins[1], A.T. Watson[1], N.K. Watson[1], M. Weber[10], S. Weisz[7], P.S. Wells[7], N. Wermes[10], M. Weymann[7], G.W. Wilson[19], J.A. Wilson[1], I. Wingerter[7], V-H. Winterer[9], N.C. Wood[13], S. Wotton[7], B. Wuensch[3], T.R. Wyatt[14], R. Yaari[24], Y. Yang[4,b], G. Yekutieli[24], T. Yoshida[22], W. Zeuner[7], G.T. Zorn[15].

[1]School of Physics and Space Research, University of Birmingham, Birmingham, B15 2TT, UK
[2]Dipartimento di Fisica dell' Università di Bologna and INFN, Bologna, 40126, Italy
[3]Physikalisches Institut, Universität Bonn, D-5300 Bonn 1, FRG

[4]Department of Physics, University of California, Riverside, CA 92521 USA
[5]Cavendish Laboratory, Cambridge, CB3 0HE, UK
[6]Carleton University, Dept of Physics, Colonel By Drive, Ottawa, Ontario K1S 5B6, Canada
[7]CERN, European Organisation for Particle Physics, 1211 Geneva 23, Switzerland
[8]Enrico Fermi Institute and Department of Physics, University of Chicago, Chicago Illinois 60637, USA
[9]Fakultät für Physik, Albert Ludwigs Universität, D-7800 Freiburg, FRG
[10]Physikalisches Institut, Universität Heidelberg, Heidelberg, FRG
[11]Queen Mary and Westfield College, University of London, London, E1 4NS, UK
[12]Birkbeck College, London, WC1E 7HV, UK
[13]University College London, London, WC1E 6BT, UK
[14]Department of Physics, Schuster Laboratory, The University, Manchester, M13 9PL, UK
[15]Department of Physics and Astronomy, University of Maryland, College Park, Maryland 20742, USA
[16]Laboratoire de Physique Nucléaire, Université de Montréal, Montréal, Quebec, H3C 3J7, Canada
[17]National Research Council of Canada, Herzberg Institute of Astrophysics, Ottawa, Ontario K1A 0R6, Canada
[18]Rutherford Appleton Laboratory, Chilton, Didcot, Oxfordshire, OX11 0QX, UK
[19]DPhPE, CEN Saclay, F-91191 Gif-sur-Yvette, France
[20]Department of Physics, Technion-Israel Institute of Technology, Haifa 32000, Israel
[21]Department of Physics and Astronomy, Tel Aviv University, Tel Aviv 69978, Israel
[22]International Centre for Elementary Particle Physics and Dept of Physics, University of Tokyo, Tokyo 113, and Kobe University, Kobe 657, Japan
[23]Brunel University, Uxbridge, Middlesex, UB8 3PH UK
[24]Nuclear Physics Department, Weizmann Institute of Science, Rehovot, 76100, Israel

[a]Present address: Dipartimento di Fisica, Università della Calabria and INFN, 87036 Rende, Italy
[b]On leave from Harbin Institute of Technology, Harbin, China
[c]Now at Applied Silicon Inc
[d]On leave from Manchester University
[e]On leave from Birmingham University
[f]and TRIUMF, Vancouver, Canada

# 1 Introduction

Studies of jet production in hadronic final states of $e^+e^-$ annihilations have proven to be a significant testing ground for Quantum Chromodynamics (QCD), the nonabelian gauge theory of the strong interaction. At large enough energies, collimated jets of hadrons reflect the underlying kinematics of the primary quarks and gluons (partons) and can be described by QCD perturbation theory. Measurements of the relative production rates of multijet events in the $e^+e^-$ continuum [1,2,3,4,5] and around the peak of the $Z^0$ resonance [6,7,8,9] result in good agreement with theoretical expectations and provide determinations of the coupling constant $\alpha_s$. The observed energy dependence of jet production rates demonstrates that $\alpha_s$ decreases with increasing energy, as predicted by the concept of asymptotic freedom (for reviews of the measurements, see [11,12,13]). Recent studies of angular correlations in 4-jet events [14,15,16] further enlarge the evidence for the nonabelian nature of QCD and thus for the existence of the gluon self coupling.

In this analysis, multijet production rates are analysed using a large sample of hadronic $Z^0$ decays to provide a precise determination of the strong coupling constant $\alpha_s(M_{Z^0})$. The data were recorded with the OPAL detector [17] at the CERN $e^+e^-$ collider LEP. Special emphasis is placed on the evaluation of systematic uncertainties, both on the experimental and on the theoretical side. Hadronic jets are defined by using four different jet recombination schemes for which the corresponding $O(\alpha_s^2)$ QCD calculations exist. Within each of these recombination schemes, the effects of the hadronisation process and of changing the renormalisation scale $\mu^2$ are studied. A comparison of the relative size of the resulting systematic uncertainties allows a judgement of which scheme is experimentally and theoretically preferred. The QCD parameter $\Lambda_{\overline{MS}}$ is determined in fits of the analytic $O(\alpha_s^2)$ QCD expressions to the corrected, differential 2-jet distributions of the data, for each of the four recombination schemes separately. This study updates our previous analysis [6], using higher data statistics and extending the discussion and evaluation of theoretical and experimental systematic uncertainties.

# 2 Jet Cross Sections and Recombination Schemes

The measurement of jet production rates requires the specification of jet resolution parameters which define, both theoretically and experimentally, resolvable jets of hadrons. In addition, jet resolution parameters ensure that jet rates are infrared safe quantities which can be calculated by QCD perturbation theory. The most commonly used jet definition requires the scaled pair mass

$$y_{ij} = M_{ij}^2/E_{cm}^2 \tag{1}$$

of each pair of resolvable jets $i$ and $j$ to exceed a certain threshold value $y_{cut}$; $E_{cm}$ is the centre of mass energy of the event. Jet pairs with $y_{ij} < y_{cut}$ are combined into a single jet. While this jet resolution parameter provides a means to compare experimental jet rates to the theoretical predictions, it also introduces ambiguities which are commonly called "recombination scheme uncertainties": the results of the calculations depend on the detailed prescription for combining two unresolvable jets into a single jet. This ambiguity arises because the $O(\alpha_s^2)$ QCD calculations are performed for massless partons, whereas a jet formed by adding the four-momenta of two previously unresolved partons is not massless. An algorithm must be chosen to deal with this mass; the freedom in selecting this algorithm is what introduces the recombination scheme uncertainty.

A number of recombination schemes has been introduced to combine two partons, with different treatments of the invariant mass of the resulting parton jet. The four most common schemes, called

"E0", "E", "p0" and "p", are defined as follows (see also [18]):

**E-scheme:** The scaled invariant mass squared of a pair of partons $i$ and $j$ is calculated from the corresponding four-vectors, $\mathbf{p_i}$ and $\mathbf{p_j}$, according to

$$y_{ij} = \frac{(\mathbf{p_i} + \mathbf{p_j})^2}{E_{cm}^2}. \tag{2}$$

If $y_{ij} < y_{cut}$, partons $i$ and $j$ are replaced by a parton jet $k$ with four-momentum

$$\mathbf{p_k} = \mathbf{p_i} + \mathbf{p_j}. \tag{3}$$

This scheme is Lorentz invariant and energy and momentum are strictly conserved. However the parton jet $k$ has a non-zero mass value which cannot consistently be accounted for in the QCD calculations.

**E0-scheme:** The invariant pair mass is defined as in Eq. 2, while the four-momentum of the recombined parton jet $k$ is calculated according to

$$\begin{aligned} E_k &= E_i + E_j \\ \vec{p}_k &= \frac{E_k}{|\vec{p}_i + \vec{p}_j|} \cdot (\vec{p}_i + \vec{p}_j). \end{aligned} \tag{4}$$

The space-component $\vec{p}_k$ is rescaled so that the vector $k$ has zero invariant mass. This scheme is not Lorentz invariant. It can be applied only in the laboratory frame and does not conserve the total momentum sum of an event.

**p-scheme:** The four-vector $\mathbf{p_k}$ is constructed such that it is has zero invariant mass, according to

$$\begin{aligned} \vec{p}_k &= \vec{p}_i + \vec{p}_j \\ E_k &= |\vec{p}_k|. \end{aligned} \tag{5}$$

While this scheme conserves the total momentum in an event, the total energy sum gradually decreases with each recombination of parton pairs and it is not Lorentz invariant.

**p0-scheme:** Jet recombination is treated as in the p-scheme; however with the following modification: the effective scaled invariant jet pair mass is calculated according to

$$y_{ij} = \frac{M_{ij}^2}{E_{vis}^2}, \tag{6}$$

where $E_{vis}$ is the actual, total energy sum of the event recalculated after each recombination. This, in contrast to the p-scheme, keeps the effective cut-off mass below which two jets are to be recombined constant, despite the decrease in total energy after each recombination.

Once a recombination scheme is chosen, the relative production rates $R_n$ of 2-, 3- and 4-jet events can be calculated in $O(\alpha_s^2)$ QCD perturbation theory. They are functions of the coupling constant $\alpha_s(\mu)$:

$$\begin{aligned} R_2 &\equiv \frac{\sigma_2}{\sigma_{tot}} = 1 + C_{2,1}(y_{cut}) \cdot \alpha_s(\mu) + C_{2,2}(y_{cut}, f) \cdot \alpha_s^2(\mu) \\ R_3 &\equiv \frac{\sigma_3}{\sigma_{tot}} = C_{3,1}(y_{cut}) \cdot \alpha_s(\mu) + C_{3,2}(y_{cut}, f) \cdot \alpha_s^2(\mu) \\ R_4 &\equiv \frac{\sigma_4}{\sigma_{tot}} = C_{4,2}(y_{cut}) \cdot \alpha_s^2(\mu), \end{aligned} \tag{7}$$

where $\sigma_{tot}$ is the total hadronic cross section, $\sigma_n$ are the cross sections for n-parton event production, $\mu$ is the renormalisation scale at which $\alpha_s$ is evaluated and $f = \mu^2/E_{cm}^2$ is the renormalisation scale factor. The $k^{th}$ order QCD coefficients for $n$-jet production, $C_{n,k}$, depend on the jet resolution parameter $y_{cut}$; in addition, the next-to-leading order coefficients $C_{2,2}$ and $C_{3,2}$ are recombination scheme dependent and exhibit an explicit dependence on the renormalisation scale factor $f$. The coupling constant $\alpha_s(\mu)$ can be written as a function of $ln(\mu^2/\Lambda^2_{\overline{MS}})$, where $\Lambda_{\overline{MS}}$ is the QCD scale parameter which must be determined by experiment. Here we use the functional form of $\alpha_s$ given in [19] to relate $\alpha_s$ and $\Lambda_{\overline{MS}}$:

$$\alpha_s(\mu) = \frac{12\pi}{(33-2\cdot N_f)\cdot ln(\frac{\mu}{\Lambda_{\overline{MS}}})^2}\cdot\left(1-6\cdot\frac{153-19\cdot N_f}{(33-2\cdot N_f)^2}\cdot\frac{ln(ln(\frac{\mu}{\Lambda_{\overline{MS}}})^2)}{ln(\frac{\mu}{\Lambda_{\overline{MS}}})^2}\right), \qquad (8)$$

with the number of active quark flavours $N_f$ equal to 5.

Recent calculations of the coefficients $C_{n,k}$ in complete second order perturbation theory are available from Kramer and Lampe [20] and from Kunszt and Nason [18]; the latter are based on the original calculations of Ellis, Ross and Terrano [21] and are carried out for the E-, E0- and p-schemes. A corresponding calculation for the p0-scheme has recently become available [22]. Therefore, in the following, we employ the calculations of Kunszt and Nason, because we wish to examine the dependence of the $\alpha_s$ determination on the recombination scheme.

# 3 Experimental Implementation of Jet Recombination Schemes

The most commonly used jet finding algorithm which is based on the invariant mass method was introduced by the JADE collaboration [1]. This algorithm defines resolvable jets of hadrons by means of a recombination scheme which is mathematically similar to the E0-scheme described above. The difference relative to the E0-scheme is that, for the JADE algorithm, two four-vectors are recombined according to Eq. 3, while the pair mass between two four-vectors $\mathbf{p_i}$ and $\mathbf{p_j}$ is calculated according to

$$M_{ij}^2 = 2\cdot E_i\cdot E_j\cdot(1-cos\Theta_{ij}), \qquad (9)$$

where $E_i$ and $E_j$ are the energies of the two particles $i$ and $j$ and $\Theta_{ij}$ is the angle between them. In this way, the approximation of neglecting explicit mass terms is made during the calculation of the pair mass while the actual recombination is done in the mathematically exact way. It can be verified that the E0- and the JADE-scheme yield identical pair masses for a given pair of four-vectors. This implies that both schemes are equivalent in $O(\alpha_s^2)$ calculations. We verified that also for the purpose of counting jet production rates in hadronic final states, where the total number of recombinations per event is of the order of 30 to 40, both schemes give identical results. However, small differences can be observed in the directions of individual jets if they consist of more than 3 particles, which is due to the fact that the JADE algorithm conserves both energy and momentum during the recombination process while the E0-algorithm violates momentum conservation.

For our analysis, we have therefore chosen to use the original JADE algorithm for the E0 scheme. We modified the same jet finder to define jets in the E-, the p- and the p0-schemes as well. For all recombination schemes in the experimental jet finder, the pair masses $y_{ij}$ are scaled by the total energy sum $E_{vis}$ of all particles in the event, rather than by the centre of mass energy $E_{cm}$ (c.f. Eq. 1). This reduces the size of the corrections for detector acceptance which are discussed below.

The differences between the four jet finders, both for the absolute jet production rates and for the sensitivity to the hadronisation process, are studied using the Jetset Monte Carlo program [25]

(version 7.2). We use the QCD parton shower mode with subsequent string hadronisation. The QCD and hadronisation parameters were optimised in a study of event shape distributions in hadronic $Z^0$ decays as described in one of our previous publications [23]. In Fig. 1, the relative production rates $R_n$ of $n$-jet events calculated from the sample of model events are displayed for different values of $y_{cut}$, both for partons at the end of the QCD shower and for particles after hadronisation. The E-scheme yields larger 3- ,4- and 5-jet rates compared to the other schemes for both the parton and the hadron distributions, while the smallest multijet rates are obtained from the p-scheme. More striking is the different sensitivity of the four schemes to the process of hadronisation: while the difference between the parton and the hadron distributions is small for the E0-scheme, as reported in previous studies [1,2,3,4,6,7,8,9,10], they are much larger for the E-scheme and of moderate but significant size for the p- and p0-schemes. This observation is true even for $y_{cut}$ values of 0.15 and larger, which correspond to jet pair masses of more than 35 GeV at $Z^0$ energies. Thus, for the comparison of data with analytic $O(\alpha_s^2)$ QCD calculations, the E0-scheme is the experimentally preferred one. The E-scheme requires large and therefore more model dependent hadronisation corrections of about 25% .

# 4 Jet Production Rates in Hadronic $Z^0$ Decays

In this study we analyse jet production rates within an event sample of 59,500 hadronic decays of $Z^0$ bosons, measured in the centre of mass energy range of $E_{cm}$ = 88.3 - 95.0 GeV. The total integrated luminosity corresponds to 3.35 $pb^{-1}$. The trigger conditions and event selection criteria are described in [24,6], respectively. Both charged and neutral particles, detected by the central tracking chambers and the electromagnetic lead glass calorimeter, are used to reconstruct jets.

In a first step of the analysis, the measured jet production rates are corrected for the limited detector acceptance and resolution, using bin-by-bin multiplication constants. The correction factors are obtained from two samples of Monte Carlo events, generated with the Jetset model, using the parameter values as discusssed above: the first sample includes initial state photon radiation, a simulation of the OPAL detector and the same event reconstruction and event selection as applied to the real data. The second sample consists of model events at the generator level including charged and neutral particles with lifetimes larger than $3 \cdot 10^{-10}$ s, without initial state radiation. The correction factors are determined by the ratio of the jet rates from the second to the first sample and are calculated separately for each recombination scheme.

The measured jet production rates, corrected for detector acceptance and resolution, are listed in Tables 1-4 and plotted in Fig.2 as a function of the jet resolution parameter $y_{cut}$. The errors in Tables 1-4 are the statistical errors of the measurements and of the correction factors. These errors are smaller than the symbol sizes in Fig. 2. The data are compared to the corresponding predictions of two different QCD shower models, both calculated at the generator level, namely Jetset (version 7.2) [25] and Herwig (version 4.3) [26], with parameters optimised in our previous work [23]. Jetset describes the data in detail for each of the recombination schemes, in the entire region of $y_{cut}$ values studied ($0.005 \leq y_{cut} \leq 0.200$), while Herwig shows a small deficiency of multijet rates within the E-scheme.

We have also verified that Jetset, after detector simulation and event selection as described above, provides a good description of the uncorrected, raw data similarly as seen in Fig. 2 for the case of the corrected data. This agreement and the good description of measured global event shape distributions in a wide range of centre of mass energies by this model [23] gives us confidence that Jetset can be used to correct the data for the effects of hadronisation. This is done in the second step of the

analysis, where the data are corrected, in a single bin-by-bin multiplication, for the effects of detector acceptance and resolution and for the hadronisation process. The corresponding correction factors are obtained in an analogous manner to the procedure described above, from the ratio of jet rates calculated from two samples of Jetset generated events. The first sample consists of the final partons at the end of the QCD shower; the second sample includes hadronisation, initial state radiation, a full simulation of the OPAL detector and the same selection procedure as applied to the data. Again, the correction factors are determined for each recombination scheme separately. We have verified that a more sophisticated correction procedure, namely a bin-by-bin correction for the detector effects plus a matrix multiplication which accounts for the migration of events between different jet classes during hadronisation, results in the same corrected jet rates to within the statistical errors.

# 5 Determinations of $\alpha_s(M_{Z^0})$ from differential 2-Jet Rates

We next determine the QCD scale parameter $\Lambda_{\overline{MS}}$ from fits of the analytic $O(\alpha_s^2)$ QCD calculations [18,22] to the experimental, differential 2-jet distributions $D_2(y)$, in a manner which is similar to that described in our previous study [6]. The distribution $D_2(y)$ is defined by ($y \equiv y_{cut}$)

$$D_2(y) = \frac{R_2(y) - R_2(y - \Delta y)}{\Delta y} \tag{10}$$

and measures the distribution of the $y_{cut}$ value of the events, for which the jet multiplicity changes from 3 to 2. The $D_2$ distributions are preferred for determinations of $\Lambda_{\overline{MS}}$ and $\mu^2$ since - in contrast to the *integral* jet rates shown in Fig. 2 - each event contributes only once. In addition, the $D_2$ distributions are largely decoupled from the effects of 4-jet event production. This is desirable because the 4-jet event rate cannot be used to fix the renormalisation scale $\mu^2$ since it is calculated in leading order perturbation theory only.

The distributions of $D_2(y)$ for the four recombination schemes, calculated from the integral jet rates after the correction for detector acceptance and resolution and for hadronisation, are listed in Table 5 and displayed in Fig. 3. The statistical errors of both the measurement and the correction factors as well as an additional systematic error, which accounts for experimental uncertainties and which is of similar size as the statistical error, are added in quadrature and given as the overall experimental error in $D_2$. The experimental uncertainties have been estimated by comparing the jet rates obtained, after correction, from two separate analyses, one which uses calorimeter information alone and one which uses charged track information alone. Within each recombination scheme, the corresponding $O(\alpha_s^2)$ QCD calculations are fitted to the data for two different treatments of the renormalisation scale $\mu^2$:

- The QCD parameter $\Lambda_{\overline{MS}}$ is determined for fixed renormalisation scale $\mu^2 = E_{cm}^2$. The fit is performed in regions of $y$ where the experimental 4-jet rate is less than 1%, i.e. for $y > 0.05$ in the p-scheme, $y > 0.06$ in the E0- and the p0-scheme and for $y > 0.08$ in the E-scheme. This restriction is motivated by the fact that $O(\alpha_s^2)$ calculations with $\mu^2 = E_{cm}^2$ do not describe the observed production rates of 4-jet events [1,2,3,4,6,10] and thus, by the overall normalisation condition $R_2 + R_3 + R_4 = 1$, must also fail to describe the 2- and 3-jet production rates in regions where $R_4 \neq 0$.

- Both $\Lambda_{\overline{MS}}$ and the renormalisation scale factor $f = \mu^2/E_{cm}^2$ are treated as free parameters and are determined in a two parameter fit. From previous studies it is known that the experimental discrimination between different choices of $\mu^2$ is possible in the region of $y_{cut} < 0.06$ [5,6,10]. A lower limit on $y_{cut}$ is still necessary, however, since $O(\alpha_s^2)$ QCD calculations predict unphysical

(i.e. negative) jet cross sections for small values of $y_{cut} < 0.01$, depending on the actual values of $\Lambda_{\overline{MS}}$ and $\mu^2$, and since they do not account for the production of 5-jet events. We therefore restrict the simultaneous fits of $\Lambda_{\overline{MS}}$ and $\mu^2$ to regions where the observed rates of 5-jet events are below 1%, i.e. to the data points with $y_{cut} > 0.02$ in the E0-, the p0- and the p-scheme and with $y_{cut} > 0.03$ in the E-scheme.

The theoretical curves for the best fit results and the ranges of $y$ values included in the fits are also displayed in Fig. 3. The values of $\Lambda_{\overline{MS}}$ and $f$ as well as the experimental errors from the fits are listed in Table 6. The results can be interpreted as follows:

1. The theoretical curves all provide a good description of the data in the regions where the fits are performed; the $\chi^2$ values are always below 1 per degree of freedom for these regions.

2. The calculations with $\mu^2 = E_{cm}^2$ ($f = 1$) do not provide a good description in the region $y < 0.08$ in the E-scheme and $y < 0.04$ in the E0-scheme, where apparently small renormalisation scales are needed to reproduce the data.

3. The resulting "optimised" scale factors $f$ are significantly different for the various recombination schemes; $f$ is smallest in the E-scheme ($f \approx 0.00004$, corresponding to $\mu \approx 0.6$ GeV at the $Z^0$ mass) and largest for the p-scheme ($f \approx 0.11$ or $\mu \approx 30$ GeV). For the E0-scheme, values of $f \approx 0.003$ or, equivalently, $\mu \approx 5$ GeV emerge, in agreement with results reported earlier [6].

4. As a direct consequence, the difference between the fitted values of $\Lambda_{\overline{MS}}$ for $f = 1$ and for $f$ as a free parameter, as well as between the corresponding theoretical curves at small values of $y$ is largest for the E-scheme and smallest for the p-scheme.

5. The results of $\Lambda_{\overline{MS}}$ for $f = 1$ differ by up to a factor of three between the four recombination schemes, but are much closer to each other if $f$ is treated as a free parameter.

There are several theoretical approaches to "optimise" or to fix the renormalisation scale of observables calculated in finite, higher order perturbation theory. Within Stevenson's principle of minimal sensitivity (PMS)[27] it is proposed that the optimal scale for each observable $O$ is found by solving the equation $dO/d\mu^2 = 0$; a requirement which is strictly fulfilled only in infinite order perturbation theory. Brodsky, Lepage and Mackenzie (BLM) [28] propose to fix the scale $\mu^2$ for a particular observable so that its next-to-leading order coefficient, like $C_{2,2}$ or $C_{3,2}$ in Eq. 7, is independent of $N_f$, the number of active fermions. For abelian theories, like Quantum Electrodynamics (QED), this is equivalent to the criterion that only vacuum-polarisation diagrams contribute to the effective coupling constant. In the method of Grunberg [29], the scale is chosen so that the next-to-leading order coefficient is zero, a method which is based on the partial equivalence of scale changes and variations of (unknown) higher order contributions; these might be chosen such that they cancel the (known) next-to-leading order coefficient. Applied to the analytic formulae of Kunszt and Nason [18] for 3-jet production rates, all these methods result in renormalisation scale factors $f$ which are significantly smaller than unity and which are much closer to the experimental fit results. This is demonstrated in Table 7, where the theoretically expected scale factors, as "optimised" for the 3-jet rates at $y_{cut} = 0.04$, are compared to the experimental fit values. For the E0-scheme, the three theoretical results are close to the experimental value of $f$. Note that the BLM method results in scale factors of 0.002 to 0.003 independent of the recombination scheme [1], while the Grunberg and the PMS methods favour scales which vary widely for different schemes, as is also observed from the experimental fits.

[1] To fix the scale according to the BLM method, the $N_f$-terms of the second order coefficient $C_{3,2}$ must be given. This is not available in [18] but has been calculated recently [30].

Thus, in the absence of a commonly accepted and unique theoretical prescription for optimising the renormalisation scale in $O(\alpha_s^2)$ QCD calculations, we choose to define the systematic uncertainty on the determination of $\alpha_s(M_{Z^0})$ due to the scale ambiguity in the following way: for each recombination scheme, we take the values of $\Lambda_{\overline{MS}}$ which are derived for the best fit results for the scale factor $f$ (see Table 6) and for $f = 1$. We then determine $\alpha_s$ at the scale $\mu^2 = M_{Z^0}^2$ from these two extreme $\Lambda_{\overline{MS}}$ values and quote the arithmetic mean as the measured value of $\alpha_s(M_{Z^0})$. The error attributed to the scale uncertainty is taken to be the (symmetric) difference between the mean and the two extreme limits.

Another systematic source of errors is the hadronisation uncertainty, which is usually studied by employing different QCD- and hadronisation models to determine hadronisation corrections for the data [18]. We adopt this procedure and repeat the entire analysis described so far, using a set of data distributions where detector and hadronisation effects are corrected by the Herwig QCD shower and cluster hadronisation program [26] with the parameter values of [23]. The resulting changes to $\alpha_s(M_{Z^0})$ turn out to be within $\pm 0.003$ and are thus of similar size to the experimental uncertainties.

We also include variations due to the value of parton virtualities to which the data are corrected, using Jetset. Our studies show that the choice of the parton shower cut-off $Q_0$, which is the parton invariant mass at which the QCD showering cascade is stopped in the model calculations and where the process of hadronisation sets in, has some influence on the resulting fit values of $\alpha_s(M_{Z^0})$. This is demonstrated in Fig. 4, where the values of $\alpha_s(M_{Z^0})$, determined from the differential $D_2$ distributions of the data, are plotted as a function of the $Q_0$ parameter used to determine the correction constants [2]. The results are determined separately for each recombination scheme and are presented for the analysis with fixed renormalisation scale (Fig. 4a) and for the simultaneous fits of both $\Lambda_{\overline{MS}}$ and $\mu^2$ (Fig. 4b). The default value of $Q_0$, for which results were quoted so far, is $Q_0 = 1$ GeV. Larger values of $Q_0$ in this figure imply that an increasing part of the (soft) QCD cascading process is included in the hadronisation correction of the data, which can also be interpreted as a variation of the influence of the higher order QCD contributions inherent to this model. The results shown in Fig.4 demonstrate that

- the result of $\alpha_s(M_{Z^0})$ determined in the E0-scheme is least sensitive to the choice of $Q_0$, while the other schemes show a significant dependence on $Q_0$.
- the $Q_0$-dependence observed for the p0-, the p- and especially the E-scheme is largely reduced in Fig. 4b, where the renormalisation scale $\mu^2$ is treated as a free parameter. This indicates that higher order QCD corrections are partly equivalent to and correlated with the scale uncertainty, as pointed out e.g. in [18].

We consider the variation of $\alpha_s(M_{Z^0})$ determined for the range of $Q_0 = 1$ GeV (the standard value in the Jetset QCD shower model) to $Q_0 = 10$ GeV (corresponding to parton virtualities of the same size or even larger than typically used in $O(\alpha_s^2)$ QCD calculations) as a further systematic uncertainty on the determination of $\alpha_s(M_{Z^0})$. The uncertainty is taken from Fig. 4b in order that it be as uncorrelated as possible with the error due to the scale uncertainty. This is done separately for each recombination scheme.

The final results for $\alpha_s(M_{Z^0})$, the experimental error, the hadronisation, the $Q_0$ and the renormalisation scale uncertainties are listed in Table 8 for each recombination scheme. The experimental and the hadronisation errors are common to all recombination schemes. The renormalisation scale uncer-

[2] The $Q_0$ parameter was varied in the event sample of generated parton final states, while the sample which includes hadronisation and detector simulation remained unchanged.

...ty dominates the overall error in both the E0- and the E-scheme and is largest in the E-scheme, while in the p0- and the p-scheme it is smaller and of similar size to the $Q_0$ uncertainty. Adding the errors in quadrature, the last column of Table 8 gives the overall errors of $\alpha_s(M_{Z^0})$.

The values of $\alpha_s(M_{Z^0})$ from the four recombination schemes agree well with each other and completely overlap in the range of their systematic uncertainties. From this we conclude that with a consistent treatment of both data and analytic calculations and within the overall error there is no additional recombination scheme uncertainty in the determination of $\alpha_s(M_{Z^0})$ from jet production rates. Since the theoretical uncertainties dominate the overall error values, and since these errors are largely uncorrelated from one recombination scheme to another, we are able to select the recombination scheme which yields the smallest overall error to obtain as our final answer

$$\alpha_s(M_{Z^0}) = 0.115 \pm 0.008,$$

which derives from the E0-, the p0- and the p-schemes. The somewhat larger central value of $\alpha_s(M_{Z^0})$ and the increased overall error of $\alpha_s(M_{Z^0})$ in the E-scheme are entirely due to the large renormalisation scale uncertainty within this scheme. According to Eq. 8, the quoted value of $\alpha_s(M_{Z^0})$ corresponds to a scale parameter $\Lambda_{\overline{MS}}$, for five active quark flavours, of

$$\Lambda^{(5)}_{\overline{MS}} = 190^{+105}_{-75}\ \text{MeV}.$$

# 6 Summary and Discussion

We have studied jet production rates in hadronic final states of $Z^0$ decays. To provide a complete evaluation of the theoretical uncertainties, we have used four different recombination schemes, which are applied in a consistent manner for both the experimental jet analysis and the corresponding analytic $O(\alpha_s^2)$ QCD calculations. Within each of the recombination schemes, hadronisation corrections and their systematic uncertainties are evaluated by using QCD shower Monte Carlo calculations. The corrections as well as the uncertainties are found to be different for each scheme. Hadronisation corrections are small (about 5%) for jets defined in the E0-scheme, but are rather large (about 25%) for the E-scheme. The model dependence of these corrections is found to be small and of similar size to the experimental uncertainties, corresponding to an error of less than 3% of the resulting value of $\alpha_s(M_{Z^0})$. The hadronisation corrections from the E-, p0- and p-schemes show an additional dependence on the choice of parton virtuality, $Q_0$, which defines the transition point between the QCD shower cascade and the hadronisation process or - equivalently - parameterises the inclusion of soft and higher order QCD effects in the hadronisation correction. The E0-scheme is again rather insensitive to this question. These results imply that the E0-scheme is preferred in experimental studies where jet production rates are to be compared with the corresponding analytic $O(\alpha_s^2)$ QCD calculations.

For the determination of the strong coupling strength, $\alpha_s(M_{Z^0})$, the data are corrected, within each recombination scheme, for detector acceptance and resolution and for the effects of hadronisation. The QCD parameter $\Lambda_{\overline{MS}}$ and the renormalisation scale $\mu^2$ are determined in fits of the corresponding $O(\alpha_s^2)$ QCD calculations of Kunszt and Nason [18] to the experimental $D_2$ distributions. The analytic expressions contain different second order correction terms for each of the recombination schemes and thus differ in their detailed predictions for jet production rates, a fact which is usually referred to as a theoretical recombination scheme ambiguity. In this analysis, the renormalisation scale is varied between $\mu^2 = E_{cm}^2$ and the best fit value of $\mu^2$, separately for each recombination scheme. The resulting difference in the fitted values of $\Lambda_{\overline{MS}}$ is included in the overall theoretical uncertainty of $\alpha_s(M_{Z^0})$.

The fit results for the scale parameter $f = \mu^2/E_{cm}^2$ and the corresponding scale uncertainties of $\Lambda_{\overline{MS}}$ are different for the various recombination schemes; the optimised values of $f$ range from $f \approx 0.113$ in the p-scheme to $f \approx 0.00004$ in the E-scheme.

For each recombination scheme, $\alpha_s(M_{Z^0})$ and its overall systematic uncertainty are determined from the corresponding range of $\Lambda_{\overline{MS}}$ obtained in these studies. The measurements are consistent with each other and completely overlap within their errors. We therefore conclude that with a consistent treatment of data and analytic calculations no recombination scheme uncertainty remains in the determination of $\alpha_s(M_{Z^0})$ from jet production rates. Since the absolute jet production rates are different in each recombination scheme, this result constitutes a new and significant test of the validity of perturbative QCD calculations and their compatibility with experimental data. The final result for $\alpha_s(M_{Z^0})$ from this analysis is

$$\alpha_s(M_{Z^0}) = 0.115 \pm 0.008,$$

where the error includes experimental as well as hadronisation and renormalisation scale uncertainties.

This result is in good agreement with our previous measurement of $\Lambda_{\overline{MS}}$ from jet production rates [6], where jets analysed with the JADE (E0-scheme) jet finder were compared to the analytic calculations of Kramer and Lampe [20]. These calculations predict jet rates similar to those of the ERT E0 scheme, as was shown in[31], and resulted in $\Lambda_{\overline{MS}}$ = (80 - 450) MeV or $\alpha_s(M_{Z^0}) = 0.117 \pm 0.015$. Our result is also in agreement with other determinations of $\alpha_s(M_{Z^0})$ from jet production rates [7,8,9] which were all based on the JADE (E0-scheme) jet finder. In our recent measurement of energy-energy correlations (EEC) and their asymmetry (AEEC) [32], we obtained values of $\alpha_s(M_{Z^0})$ which also agree well with the results of this analysis: the EEC resulted [3] in $\alpha_s(M_{Z^0}) = 0.124 \pm 0.012$ and the AEEC gave $\alpha_s(M_{Z^0}) = 0.117 \pm 0.009$, where the respective experimental and theoretical errors are added in quadrature. While the result from the AEEC is largely independent from changes in the renormalisation scale, the increased value and error range of $\alpha_s(M_{Z^0})$ from the EEC are mainly due to the scale uncertainty — similar to the case of the jet rates analysis using the E recombination scheme which is presented above.

We conclude that $\alpha_s(M_{Z^0})$, in second order perturbation theory, is consistently measured to be around 0.115, with total systematic uncertainties of less than 10%. The current size of errors is mainly dominated by theoretical uncertainties. Therefore higher order QCD calculations, either in complete third order or in the next-to-leading logarithm approximation to all orders of perturbation theory (e.g. as recently reported in [33]), are indispensable in order to further improve the precision of experimental determinations of $\alpha_s(M_{Z^0})$.

**Acknowledgements.** We are grateful for the many motivating and helpful discussions with G. Altarelli, Z. Kunszt and P. Nason. It is a pleasure to thank the SL Division for the efficient operation of LEP and their continuing close cooperation with our experimental group. In addition to the support staff at our own institutions we are pleased to acknowledge the following: The Bundesministerium für Forschung und Technologie, FRG, The Department of Energy, USA, The Institut de Recherche Fondamentale du Commissariat a l'Energie Atomique, The Israeli Ministry of Science, The Minerva Gesellschaft, The National Science Foundation, USA, The Natural Sciences and Engineering Research Council, Canada, The Japanese Ministry of Education, Science and Culture (the Monbusho) and a grant under the Monbusho International Science Research Program, The American Israeli Bi-national Science Foundation, The Science and Engineering Research Council, UK and The A. P. Sloan Foundation.

[3] The EEC result quoted here was calculated including the renormalisation scale uncertainty between $\mu^2 = E_{cm}^2$ and its best experimental fit result, in a similar manner as done in this analysis, from the values presented in [32].

## References


[1] JADE collab., W. Bartel et al., Phys. C33 (1986), 23;
JADE collab., S. Bethke et al., Phys. Lett. B213 (1988), 235.

[2] TASSO-collab., W. Braunschweig et al., Phys. Lett. B214 (1988), 286.

[3] AMY collab., I. Park et al., Phys. Rev. Lett. 62 (1989), 1713.

[4] Mark-II collab., S. Bethke et al., Z. Phys. C43 (1989), 325.

[5] S. Bethke, Z. Phys. C43 (1989), 331.

[6] OPAL collab., M.Z. Akrawy et al., Phys. Lett. B235 (1990) 389.

[7] Mark-II collab., S. Komamiya et al., Phys. Rev. Lett. 64 (1990) 987.

[8] DELPHI collab., P. Abreu et al., CERN-EP/90-89.

[9] L3 collab., B. Adeva et al., L3 preprint 11 (1990).

[10] JADE collab., N. Magnussen, L. Smolik et al., DESY 90-089.

[11] S. Bethke, Proc. of the XXV$^{th}$ Rencontre de Moriond, Les Arcs (France), March 1990;
Heidelberg preprint HD-PY 90/3.

[12] J. Drees, Proc. of the Neutrino-90 Conference, CERN, Geneva, June 1990.

[13] M. Jacob, Proc. of the XXV$^{th}$ Int. Conf. on High Energy Physics, Singapore, August 1990.

[14] AMY collab., I. Park et al., Phys. Rev. Lett. 62 (1989), 1713.

[15] OPAL collab., M.Z. Akrawy et al., CERN-EP/90-97.

[16] L3 collab., B. Adeva et al., L3 preprint 12 (1990).

[17] OPAL Technical Proposal (1983), CERN/LEPC/83-4;
OPAL collab., K. Ahmet et al., CERN-PPE/90-114; submitted to Nucl. Instr. and Meth.

[18] Z.Kunszt and P.Nason [conv.], in "Z Physics at LEP 1" (eds. G.Altarelli, R.Kleiss and C.Verzegnassi ), CERN 89-08 (1989).

[19] Review of Particle Properties, Phys. Lett. B204 (1988), 96.

[20] G. Kramer, B. Lampe, J. Math. Phys. 28 (1987), 945;
DESY 86-103; DESY 86-119.

[21] R.K. Ellis, D.A. Ross and A.E. Terrano, Nucl. Phys. B178 (1981), 421.

[22] P. Nason, private communication.

[23] OPAL collab., M.Z. Akrawy et al., Z. Phys. C47 (1990) 505.

[24] OPAL collab., M.Z. Akrawy et al., Phys. Lett. B231 (1989), 530;
OPAL collab., M.Z. Akrawy et al., Phys. Lett. B235 (1990), 379.

[25] T. Sjöstrand, Comp. Phys. Comm. 39 (1986), 347;
T. Sjöstrand, Comp. Phys. Comm. 43 (1987 ), 367;
M. Bengtsson and T. Sjöstrand, Nucl. Phys. B289 (1987), 810.

[26] G. Marchesini and B.R. Webber, Nucl. Phys. B310 (1988) 461;
G. Marchesini and B.R. Webber, Cavendish-HEP-88/7.

[27] P.M. Stevenson, Phys. Rev. D16 (1981) 2916

[28] S.J. Brodsky, G.P. Lepage and P.B. Mackenzie, Phys. Rev. D28 (1983) 228.

[29] G. Grunberg, Phys. Lett. B95 (1980) 70.

[30] N. Magnoli, P. Nason and R. Rattazzi, CERN-TH 5844/90.

[31] G. Kramer and N. Magnussen, DESY 90-080 (1990).

[32] OPAL collab., M.Z. Akrawy et al., CERN-PPE/90-121.

[33] S. Catani, G. Turnock, B.R. Webber and L. Trentadue, Cavendish-HEP-90/16.

| $y_{cut}$ | $R_2$ | $R_3$ | $R_4$ | $R_5$ |
|---|---|---|---|---|
| 0.005 | 13.03±0.22 | 41.88±0.35 | 31.99±0.40 | 13.09±0.32 |
| 0.010 | 26.24±0.30 | 50.73±0.40 | 19.57±0.36 | 3.46±0.19 |
| 0.015 | 36.27±0.34 | 49.93±0.41 | 12.66±0.31 | 1.14±0.12 |
| 0.020 | 43.97±0.35 | 47.18±0.43 | 8.42±0.26 | 0.43±0.08 |
| 0.030 | 55.69±0.35 | 39.81±0.42 | 4.39±0.21 | 0.11±0.05 |
| 0.040 | 63.90±0.35 | 33.82±0.41 | 2.26±0.15 | — |
| 0.050 | 70.15±0.33 | 28.59±0.39 | 1.26±0.11 | — |
| 0.060 | 75.03±0.32 | 24.34±0.36 | 0.63±0.08 | — |
| 0.080 | 81.55±0.28 | 18.27±0.33 | 0.18±0.05 | — |
| 0.100 | 86.15±0.25 | 13.79±0.30 | — | — |
| 0.120 | 89.75±0.22 | 10.25±0.26 | — | — |
| 0.140 | 92.51±0.20 | 7.49±0.23 | — | — |
| 0.170 | 95.37±0.16 | 4.63±0.18 | — | — |
| 0.200 | 97.27±0.12 | 2.73±0.14 | — | — |

**Table 1.** Experimental n-jet event production rates, $R_n$, in % of the total hadronic cross section, analysed in the **E0** recombination scheme. The data are corrected for the final acceptance and resolution of the detector and for initial state photon radiation. No corrections for hadronisation effects are applied.

| $y_{cut}$ | $R_2$ | $R_3$ | $R_4$ | $R_5$ |
|---|---|---|---|---|
| 0.005 | 0.14±0.02 | 7.26±0.14 | 33.58±0.34 | 59.01±0.58 |
| 0.010 | 1.13±0.05 | 31.79±0.30 | 43.12±0.46 | 23.96±0.52 |
| 0.015 | 4.45±0.11 | 49.08±0.37 | 36.29±0.50 | 10.18±0.37 |
| 0.020 | 9.41±0.17 | 57.91±0.40 | 27.70±0.47 | 4.97±0.29 |
| 0.030 | 21.40±0.25 | 61.23±0.46 | 16.19±0.41 | 1.18±0.15 |
| 0.040 | 33.20±0.30 | 57.05±0.48 | 9.39±0.33 | 0.36±0.09 |
| 0.050 | 43.32±0.33 | 50.86±0.49 | 5.68±0.26 | 0.14±0.16 |
| 0.060 | 51.59±0.33 | 45.06±0.49 | 3.35±0.21 | — |
| 0.080 | 64.60±0.32 | 34.02±0.45 | 1.38±0.17 | — |
| 0.100 | 73.72±0.30 | 25.73±0.42 | 0.55±0.15 | — |
| 0.120 | 80.35±0.27 | 19.47±0.38 | 0.18±0.15 | — |
| 0.140 | 85.04±0.24 | 14.96±0.34 | — | — |
| 0.170 | 90.36±0.20 | 9.64±0.29 | — | — |
| 0.200 | 93.86±0.16 | 6.14±0.23 | — | — |

**Table 2.** Experimental n-jet event production rates, $R_n$, in % of the total hadronic cross section, analysed in the **E** recombination scheme. The data are corrected for the final acceptance and resolution of the detector and for initial state photon radiation. No corrections for hadronisation effects are applied.

| $y_{cut}$ | $R_2$ | $R_3$ | $R_4$ | $R_5$ |
|---|---|---|---|---|
| 0.005 | 17.97±0.28 | 44.16±0.39 | 27.62±0.39 | 10.25±0.29 |
| 0.010 | 33.44±0.35 | 47.99±0.41 | 15.87±0.33 | 2.70±0.17 |
| 0.015 | 43.62±0.37 | 45.33±0.42 | 10.17±0.28 | 0.88±0.11 |
| 0.020 | 51.17±0.37 | 41.64±0.42 | 6.79±0.24 | 0.40±0.09 |
| 0.030 | 62.38±0.37 | 34.07±0.40 | 3.50±0.18 | — |
| 0.040 | 69.26±0.35 | 28.88±0.39 | 1.86±0.13 | — |
| 0.050 | 74.56±0.33 | 24.35±0.37 | 1.09±0.11 | — |
| 0.060 | 78.84±0.32 | 20.69±0.35 | 0.47±0.07 | — |
| 0.080 | 84.64±0.28 | 15.23±0.30 | 0.13±0.04 | — |
| 0.100 | 88.60±0.25 | 11.36±0.27 | — | — |
| 0.120 | 91.33±0.21 | 8.67±0.25 | — | — |
| 0.140 | 93.75±0.19 | 6.25±0.21 | — | — |
| 0.170 | 96.03±0.15 | 3.97±0.17 | — | — |
| 0.200 | 97.65±0.12 | 2.35±0.13 | — | — |

**Table 3.** Experimental n-jet event production rates, $R_n$, in % of the total hadronic cross section, analysed in the **p0** recombination scheme. The data are corrected for the final acceptance and resolution of the detector and for initial state photon radiation. No corrections for hadronisation effects are applied.

| $y_{cut}$ | $R_2$ | $R_3$ | $R_4$ | $R_5$ |
|---|---|---|---|---|
| 0.005 | 18.94±0.29 | 45.37±0.39 | 26.85±0.39 | 8.84±0.27 |
| 0.010 | 34.72±0.35 | 48.44±0.41 | 14.89±0.32 | 1.95±0.15 |
| 0.015 | 45.53±0.38 | 44.84±0.42 | 8.98±0.26 | 0.65±0.09 |
| 0.020 | 53.35±0.38 | 40.70±0.42 | 5.77±0.22 | 0.17±0.05 |
| 0.030 | 64.24±0.37 | 32.95±0.40 | 2.78±0.16 | — |
| 0.040 | 71.62±0.35 | 27.02±0.38 | 1.36±0.12 | — |
| 0.050 | 77.12±0.33 | 22.32±0.35 | 0.56±0.07 | — |
| 0.060 | 81.26±0.31 | 18.49±0.33 | 0.25±0.05 | — |
| 0.080 | 86.94±0.26 | 13.01± 0.28 | — | — |
| 0.100 | 90.82±0.23 | 9.19±0.24 | — | — |
| 0.120 | 93.81±0.19 | 6.19±0.20 | — | — |
| 0.140 | 95.66±0.16 | 4.34±0.17 | — | — |
| 0.170 | 97.69±0.12 | 2.31±0.12 | — | — |
| 0.200 | 98.81±0.08 | 1.19±0.09 | — | — |

**Table 4.** Experimental n-jet event production rates, $R_n$, in % of the total hadronic cross section, analysed in the **p** recombination scheme. The data are corrected for the final acceptance and resolution of the detector and for initial state photon radiation. No corrections for hadronisation effects are applied.

| $y$ | $\Delta y$ | $D_2$ (E0-scheme) | $D_2$ (E-scheme) | $D_2$ (p0-scheme) | $D_2$ (p-scheme) |
|---|---|---|---|---|---|
| 0.02 | 0.01 | 16.80±0.41 | 16.16±0.46 | 17.78±0.43 | 18.60±0.44 |
| 0.03 | 0.01 | 11.38±0.44 | 12.09±0.51 | 12.09±0.47 | 11.92±0.46 |
| 0.04 | 0.01 | 8.37±0.45 | 9.29±0.53 | 7.84±0.46 | 8.25±0.46 |
| 0.05 | 0.01 | 6.55±0.44 | 7.55±0.52 | 5.84±0.44 | 6.30±0.44 |
| 0.06 | 0.01 | 5.19±0.42 | 5.77±0.50 | 5.02±0.42 | 4.72±0.42 |
| 0.08 | 0.02 | 3.64±0.19 | 4.78±0.24 | 3.32±0.20 | 3.26±0.19 |
| 0.10 | 0.02 | 2.39±0.18 | 3.29±0.22 | 2.12±0.17 | 2.17±0.16 |
| 0.12 | 0.02 | 1.87±0.16 | 2.51±0.19 | 1.53±0.15 | 1.69±0.14 |
| 0.14 | 0.02 | 1.43±0.14 | 1.79±0.17 | 1.31±0.14 | 1.09±0.12 |
| 0.17 | 0.03 | 0.99±0.08 | 1.36±0.10 | 0.84±0.08 | 0.77±0.07 |
| 0.20 | 0.03 | 0.65±0.06 | 0.98±0.08 | 0.58±0.06 | 0.47±0.05 |

**Table 5.** Measured 2-jet distributions $D_2(y)$ (c.f. Eq. 10) for 4 different jet recombination schemes, corrected for detector acceptance, initial state photon radiation and hadronisation effects to a minimal parton virtuality of $Q_0 = 1$ GeV.

| Fit | E0-scheme | E-scheme | p0-scheme | p-scheme |
|---|---|---|---|---|
| $\Lambda_{\overline{MS}}$ ($f$=1) | $287^{+45}_{-41}$ | $650^{+90}_{-84}$ | $228^{+45}_{-40}$ | $209^{+37}_{-34}$ |
| $\Lambda_{\overline{MS}}$ | $114 \pm 13$ | $111 \pm 11$ | $147^{+20}_{-17}$ | $154^{+39}_{-20}$ |
| $f$ | $0.0032^{+0.0014}_{-0.0008}$ | $0.00004 \pm 0.00001$ | $0.053^{+0.172}_{-0.031}$ | $0.113^{+0.701}_{-0.113}$ |

**Table 6.** Fit results of $\Lambda_{\overline{MS}}$ for fixed renormalisation scale factor $f = \mu^2/E_{cm}^2 \equiv 1$ and for the simultaneous determination of $\Lambda_{\overline{MS}}$ and $f$ in the differential $D_2$ distributions; for details see text.

| | E0-scheme | E-scheme | p0-scheme | p-scheme |
|---|---|---|---|---|
| $f$ (BLM) | 0.0024 | 0.0035 | 0.0020 | 0.0019 |
| $f$ (PMS) | 0.0060 | 0.00029 | 0.028 | 0.045 |
| $f$ (Grunberg) | 0.0081 | 0.00036 | 0.034 | 0.056 |
| $f$ (exp.) | $0.0032^{+0.0014}_{-0.0008}$ | $0.00004 \pm 0.00001$ | $0.053^{+0.172}_{-0.031}$ | $0.113^{+0.701}_{-0.113}$ |

**Table 7:** Optimised renormalisation scale factors $f$, calculated for the jet production rates at $y_{cut} = 0.04$ according to the BLM [28], the PMS [27] and the Grunberg [29] method and compared to the experimental fit results of $f$ from the $D_2$ distributions.

| Scheme | $\alpha_s(M_{Z^0})$ | $\Delta\alpha_s$ (exp.) | $\Delta\alpha_s$ (had.) | $\Delta\alpha_s$ ($Q_0$) | $\Delta\alpha_s$ (scale) | $\Delta\alpha_s$ (tot.) |
|---|---|---|---|---|---|---|
| E0 | 0.115 | $\pm$0.003 | $\pm$0.003 | $\pm$0.003 | $\pm$0.007 | $\pm$0.009 |
| E | 0.123 | $\pm$0.003 | $\pm$0.003 | $\pm$0.003 | $\pm$0.014 | $\pm$0.015 |
| p0 | 0.115 | $\pm$0.003 | $\pm$0.003 | $\pm$0.004 | $\pm$0.005 | $\pm$0.008 |
| p | 0.115 | $\pm$0.003 | $\pm$0.003 | $\pm$0.006 | $\pm$0.004 | $\pm$0.008 |

**Table 8.** Final results of $\alpha_s(M_{Z^0})$ for different recombination schemes.

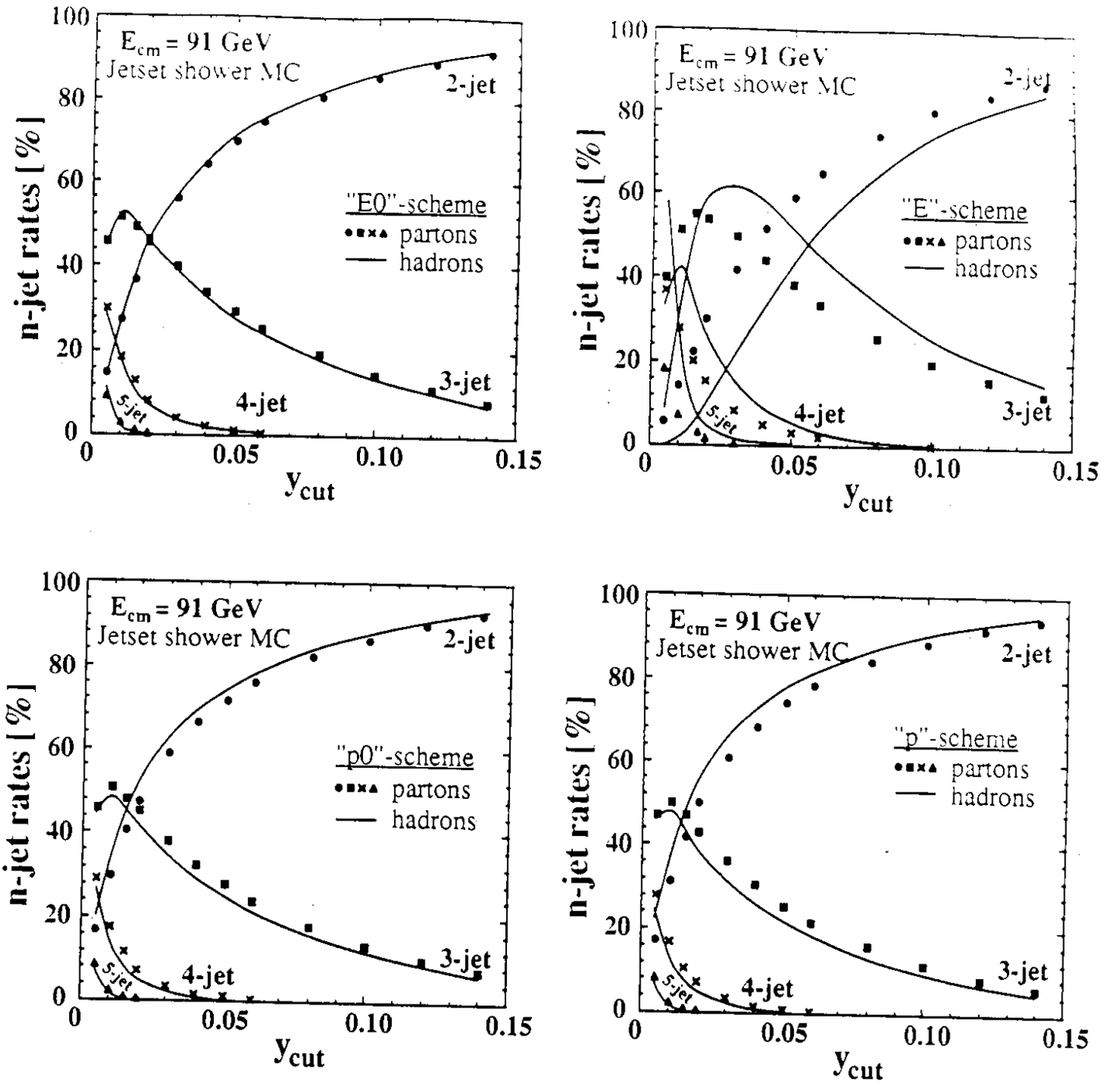


Fig. 1. Relative production rates of $n$-jet events, determined from model calculations before and after the hadronisation process for four different jet recombination schemes, as a function of the jet resolution parameter $y_{cut}$.

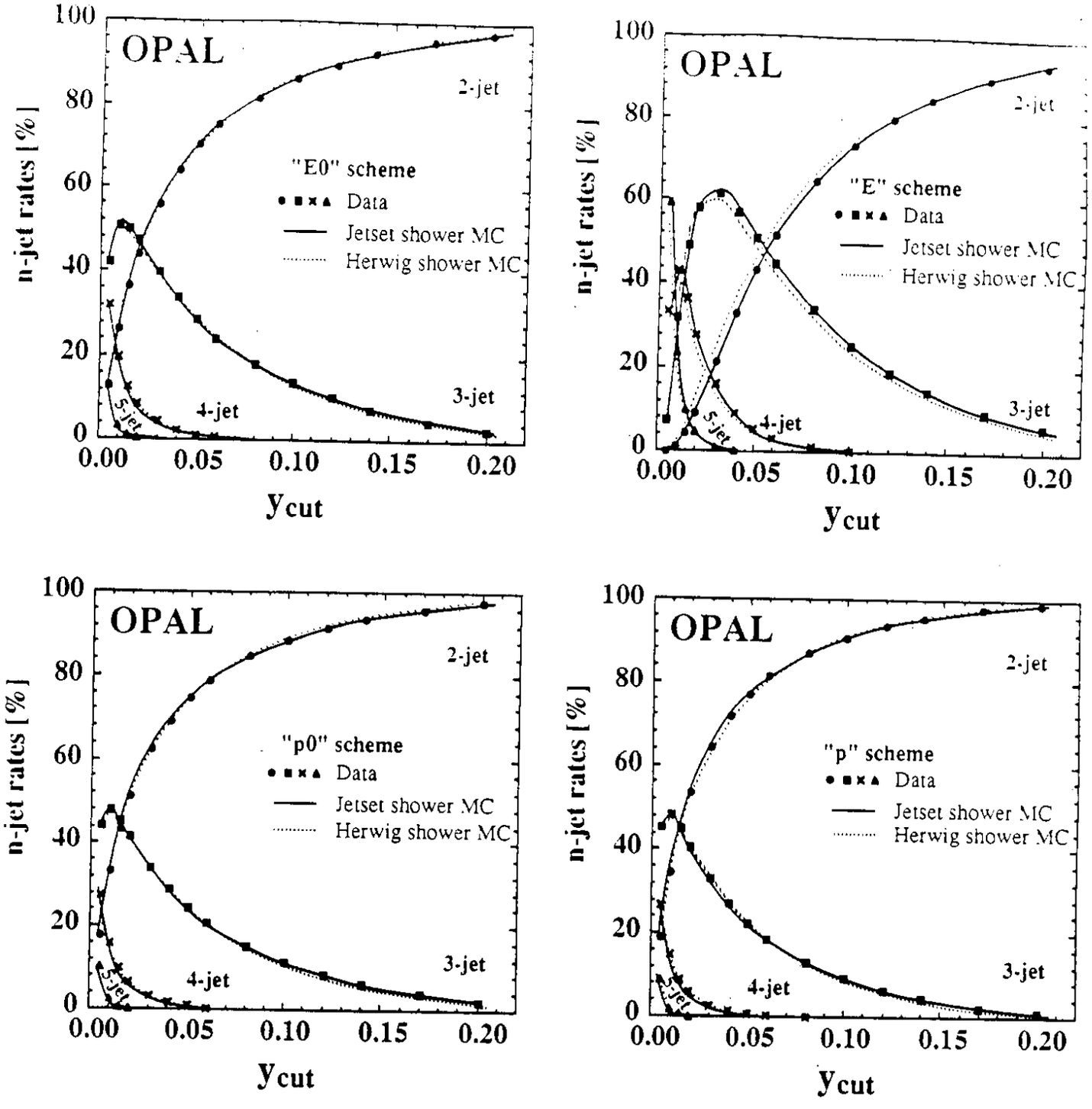


Fig. 2. Relative production rates of $n$-jet events, observed at $E_{cm} = 91$ GeV as a function of $y_{cut}$, compared to two different QCD shower model calculations. The data are corrected for detector resolution and acceptance and for initial state photon radiation.

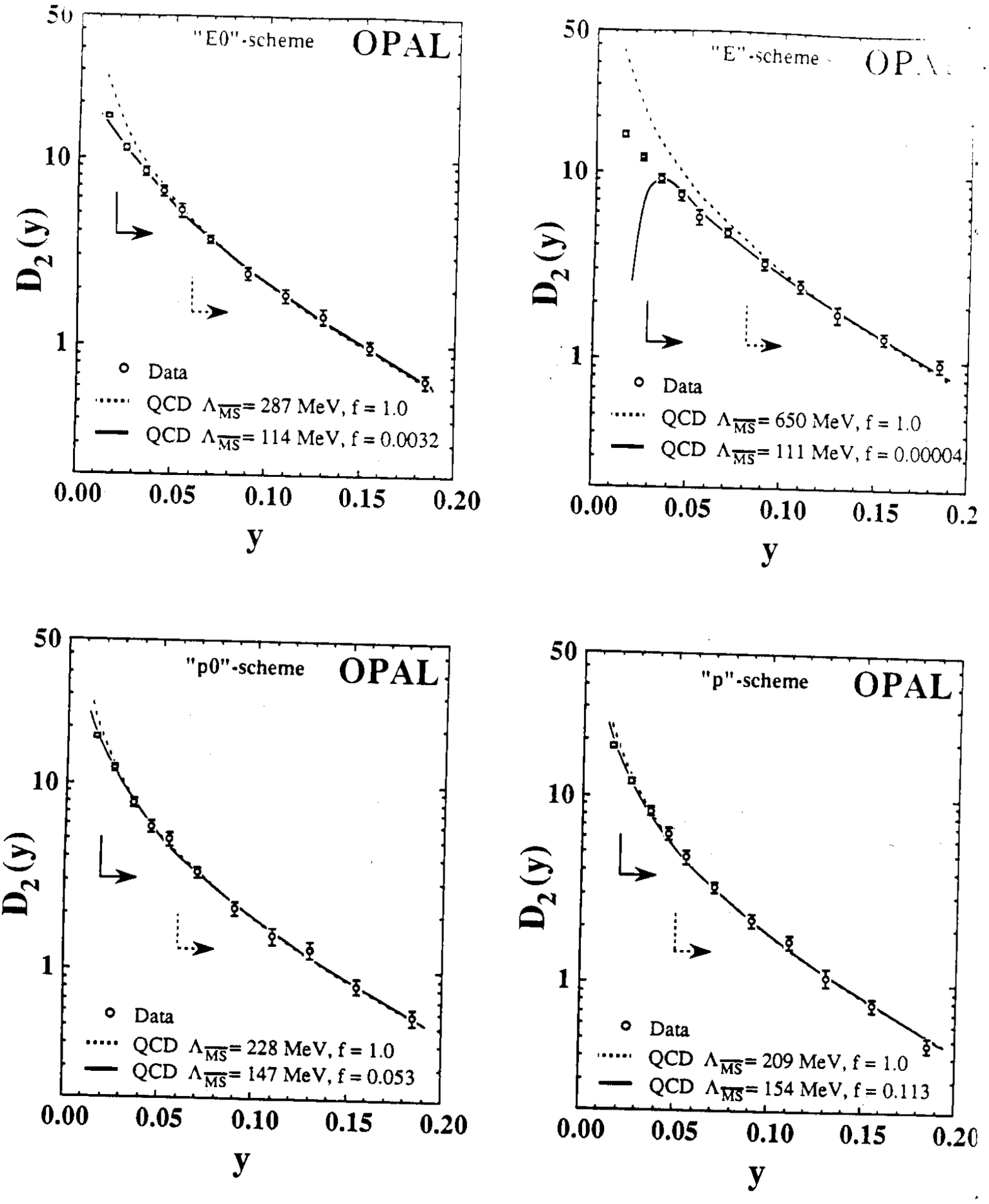


Fig. 3. Measured distributions of $D_2(y)$, corrected for detector acceptance and hadronisation effects, compared to the corresponding analytic $O(\alpha_s^2)$ QCD calculations. The QCD parameters are taken from the fit results of $\Lambda_{\overline{MS}}$ with $f = 1$ and of $\Lambda_{\overline{MS}}$ and $\mu^2$ in the regions of $y$ indicated by the arrows.

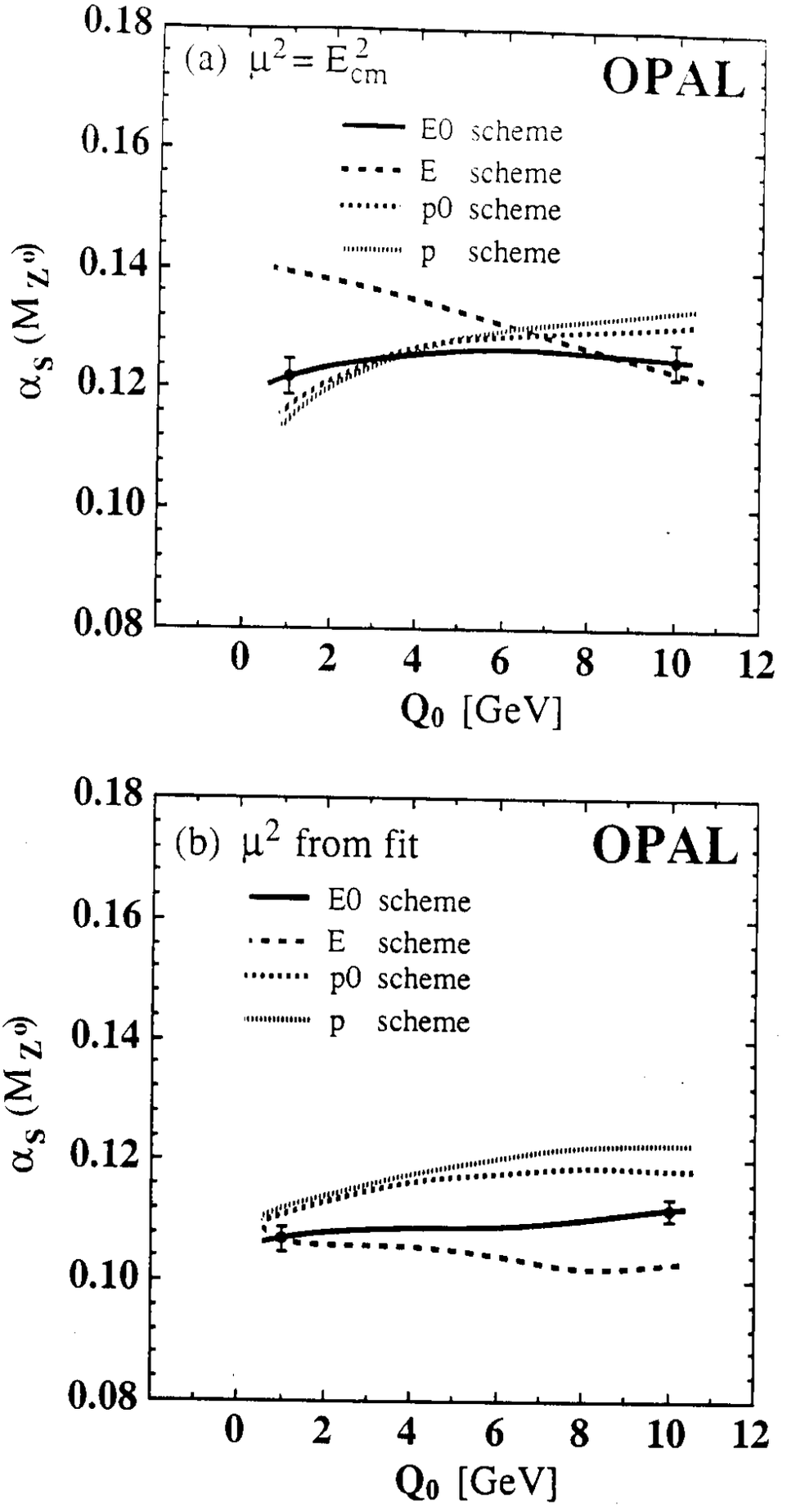


**Fig. 4.** Values of $\alpha_s(M_{Z^0})$ calculated from fit results of $\Lambda_{\overline{MS}}$, for $\mu^2 = E^2_{cm}$ (a) and for $\mu^2$ as a free parameter (b), as a function of the parton virtuality $Q_0$ to which the data are corrected. The errors displayed for the E0 results represent the experimental errors of the fits.



Imprimé au CERN. Prix : 0.70 Fr.